In: GLOBECOM 2024 - 2024 IEEE Global Communications Conference, 8-12 Dec 2024, Cape Town, South Africa, pp. 1617-1622
DOI:10.1109/globecom52923.2024.10901660

Deep Learning Based Secure Transmissions for the UAV-RIS Assisted Networks: Trajectory and Phase Shift Optimization

Jiawei Li[1], Dawei Wang[1], Jiankang Zhang[2], Osama Alfarraj[3], Yixin He[4],
Saba Al-Rubaye[5], Keping Yu[3,6] and Shahid Mumtaz[7]
[1]School of Electronics and Information, Northwestern Polytechnical University, Xi'an, 710072, China
[2]Department of Computing and Informatics, Bournemouth University, UK
[3] Department of Computer Science, Community College, King Saud University, Riyadh 11437, Saudi Arabia
[4]College of Information Science and Engineering, Jiaxing University, Jiaxing, 314001, China
[5]School of Aerospace, Transport, and Manufacturing, Cranfield University, UK
[6]School of Science and Engineering, Hosei University, Tokyo 184-8584, Japan
[7] Department of Applied Informatics, Silesian University of Technology, Akademicka 16 44-100 Gliwice, Poland
and Departement of Computer Sciences, Nottingham Trent University, UK
Email: lijw@mail.nwpu.edu.cn, wangdw@nwpu.edu.cn, jzhang3@bournemouth.ac.uk, oalfarraj@ksu.edu.sa,
yixinhe@zjxu.edu.cn, s.alrubaye@cranfield.ac.uk, KepingYu@ksu.edu.sa, dr.shahid.mumtaz@ieee.org

***Abstract*—This paper investigates the secure transmissions in the Unmanned Aerial Vehicle (UAV) communication network facilitated by a Reconfigurable Intelligent Surface (RIS). In this network, the RIS acts as a relay, forwarding sensitive information to the legitimate receiver while preventing eavesdropping. We optimize the positions of the UAV at different time slots, which gives another degree to protect the privacy information. For the proposed network, a secrecy rate maximization problem is formulated. The non-convex problem is solved by optimizing the RIS's phase shifts and UAV trajectory. The RIS phase shift optimization problem is converted into a series of subproblems, and a non-linear fractional programming approach is conceived to solve it. Furthermore, the first-order taylor expansion is employed to transform the UAV trajectory optimization into convex function, and then we use the deep Q-network (DQN) method to obtain the UAV's trajectory. Simulation results show that the proposed scheme enhances the secrecy rate by 18.7% compared with the existing approaches.**

***Index Terms*—Unmanned aerial vehicle, reconfigurable intelligent surface, security.**

I. Introduction

The World Health Organization (WHO) defines e-health as "a digital ecosystem that uses information and communication technology (ICT) to support health in the cost-effective and safe manner". The appropriate use of e-health ensures the integrity of an individual's health information and contributes to the development of health education through privacy protection. As ICT is becoming more and more sophisticated, people have higher demands on secure, ultra-reliable, and low-latency communication requirements [1]. Typically, the communication links are vulnerable to being blocked by obstacles. UAVs have high maneuverability and deployment flexibility, so they can restore communication links and improve the accuracy of information transmission. However, due to the light-of-sight transmission links in the UAV networks, private information can easily be captured by the eavesdroppers, resulting in the risk of information leakage.

The physical layer security (PLS) technique is a promising solution to protect privacy information. To prevent information leakage, the authors of [2] and [3] modeled a UAV-assisted communication network, thereby optimizing the movement of UAV and maximizing the secrecy rate. Besides, some researchers have introduced reconfigurable intelligent surface (RIS) to protect the primary information [4]. The author of [5] introduced RIS and derived the mathematical expression of the active beamforming vector to optimize the two-dimensional (2D) UAV trajectory. The authors of [6] and [7] proposed to deploy RIS on the surface of the building as a relay. They formulated a Markov decision process to improve secrecy performance, while deep Q-learning(DQL) was used to maximize the secrecy rate. The authors in [8]–[10] applied successive convex approximation (SCA) algorithm, and presented an alternate framework for optimization to guarantee information security.

All the above works investigated information security with PLS technique. However, the information secure transmission assisted by the UAV equipped with a RIS has not been fully studied, especially in scenarios involving dynamic UAVs. Since the RIS integrates numerous tightly arranged electro-

This work was supported in part by the National Natural Science Foundation of China under Grants 62271399 and 62206221, in part by National Key Research and Development Program of China under Grant 2020YFB1807003, in part by Foundation of the Science, Technology, and Innovation Commission of Shenzhen Municipality under Grant JCYJ20190806160218174, in part by Zhejiang Provincial Natural Science Foundation of China under Grant LQ24F010003, in part by the Distinguished Scientist Fellowship Program (DSFP) at King Saud University, Riyadh, Saudi Arabia, and in part by the Bournemouth University Qualiy research funding: Flying ad-hoc networking and its applications. *(Corresponding author: Dawei Wang).*

magnetic reflective elements that can intelligently configure the wireless communication environment by changing its location, the system can acquire another degree of freedom to protect private information. Inspired by the above, we examine secure transmission in UAV networks aided by the RIS. Explicitly, we optimize RIS phase shifts and the trajectory of UAV for secrecy rate maximization. The main contributions are summarized below.

- For the RIS-assisted UAV network, which includes a remote base station (Alice), a legitimate receiver (Bob), and an eavesdropper, a RIS-assisted UAV is employed to protect private information. We formulate an optimization problem for maximizing the secrecy rate by respectively optimizing the RIS phase shift and UAV trajectory.
- We decouple the secrecy rate maximization problem into two subproblems: optimizing the RIS phase shifts and UAV trajectory. For the first phase shifts problem, we use a non-linear fractional programming approach, thereby obtaining optimal phase shifts. A first-order taylor expansion is employed to convert the non-convex UAV trajectory problem into convex forms, and then we apply the deep Q-Network (DQN) algorithm to determine the optimal UAV trajectory.
- The simulation results substantiate that our proposed scheme increases secrecy rate by 18.7% and ensures secure communication in comparison with the current works.

II. System Model

We investigate a UAV communication network facilitated by RIS, as depicted in Fig. 1. The network has a base station (Alice), a legitimate receiver (Bob) and an eavesdropper (Eve). The eavesdropper can easily acquire confidential information transmitted to legitimate receiver due to the wireless channel's broadcast property. For private information protection, the RIS-equipped UAV is utilized as an air relay to ensure legitimate transmission and reduce information leakage.

In this network, Alice, Bob, and Eve are located on the ground. RIS has M reflecting elements and can change its location and phase shift depending on the movement of the UAV. We use a 3D coordinate system, and the horizontal positions of Alice, Bob, and Eve are expressed as $\mathbf{Z}_A = [x_A, y_A]^T, \mathbf{Z}_B = [x_B, y_B]^T, \mathbf{Z}_E = [x_E, y_E]^T$. The flight time T is divided into N time slots. The UAV's horizontal position at n-th time slot is defined as $\mathbf{Z}[n] = [x_n, y_n]^T$, and the initial altitude of UAV is H_{uav}.

A. Communication Channel Model

There are M reflective elements on the RIS and the elements are arranged in a square, which is considered as a uniform planar array (UPA) with $M = P \times P$. RIS is located in the **xoz** plane, then RIS's antenna array response is given by

$$\mathbf{a}\left(\theta[n], \phi[n]\right) = \frac{1}{\sqrt{M}}[1, e^{-j\frac{2\pi d}{\lambda}(\sin\phi\sin\theta+\cos\theta)}, \cdots, e^{-j\frac{2\pi d}{\lambda}\left((\sqrt{M}-1)\sin\phi\sin\theta+(\sqrt{M}-1)\cos\theta\right)}]^T, \quad (1)$$

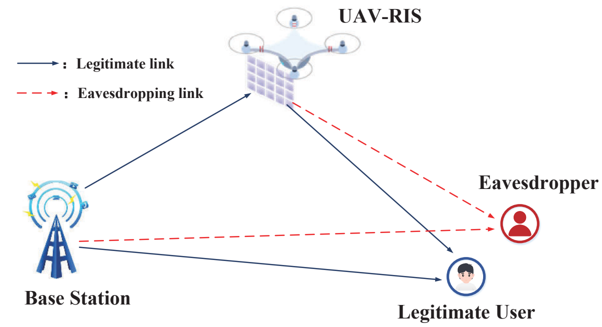

Fig. 1. A RIS-assisted UAV secure transmission network.

where antenna response vectors for the **x** and **z** axes can be denoted as

$$\mathbf{a}_x\left(\theta, \phi\right) = \frac{1}{\sqrt{P}}[1, e^{-j\frac{2\pi d}{\lambda}\sin\phi\sin\theta}, \cdots, e^{-j\frac{2\pi d}{\lambda}(P-1)\sin\phi\sin\theta}]^T, \quad (2)$$

$$\mathbf{a}_z\left(\theta, \phi\right) = \frac{1}{\sqrt{P}}[1, e^{-j\frac{2\pi d}{\lambda}\cos\phi}, \cdots, e^{-j\frac{2\pi d}{\lambda}(\sqrt{M}-1)\cos\phi}]^T, \quad (3)$$

In addition, θ is the horizontal azimuth angle and ϕ is the elevation angle. The wavelength is λ, and d_{ui} $(i \in \{a, b, e\})$ is the distance between UAV and the communication devices on the ground, which can be denoted as

$$\begin{cases} \cos\phi = \frac{H_{uav}}{d_{ui}}, \\ \sin\phi\sin\theta = \frac{x_i - x_n}{d_{ui}}, \\ d_{ui} = \sqrt{(x_n - x_i)^2 + (y_n - y_i)^2 + H_{uav}^2}, \end{cases} \quad (4)$$

Thus, the channel from RIS to the ground devices is represented as

$$\mathbf{h}_{ui}[n] = \sqrt{\rho_0 d_{ui}^{-\alpha_1}}\left(\zeta_1 \cdot \mathbf{h}_{ui}^{LOS}[n] + \zeta_2 \cdot \mathbf{h}_{ui}^{NLOS}[n]\right), \quad (5)$$

where $\zeta_1 = \sqrt{\frac{L}{L+1}}$, $\zeta_2 = \sqrt{\frac{1}{L+1}}$. ρ_0 represents the path loss at a reference distance of 1 m and α_1 denotes the air-to-ground path loss. The air-to-ground channel is dominated by the LoS component and follows Rician fading, with L denoting the Rician factor. The LoS channel is denoted as

$$\begin{aligned} \mathbf{h}_{ui}^{LOS}[n] &= \sqrt{M} \cdot \mathbf{a}_x\left(\theta, \varphi\right) \otimes \mathbf{a}_z\left(\theta, \varphi\right) \\ &= [1, e^{-j\frac{2\pi d}{\lambda}\sin\phi\sin\theta}, \cdots, e^{-j\frac{2\pi d}{\lambda}(P-1)\sin\phi\sin\theta}]^T \\ &\quad \otimes [1, e^{-j\frac{2\pi d}{\lambda}\cos\phi}, \cdots, e^{-j\frac{2\pi d}{\lambda}(\sqrt{M}-1)\cos\phi}]^T. \end{aligned} \quad (6)$$

The NLoS channel component $\tilde{\mathbf{h}}_{ui}^{NLOS}[n] \in \mathbb{C}^{M\times 1}$ can be viewed as the complex Gaussian distribution, i.e., $\tilde{\mathbf{h}}_{ui}^{NLOS}[n] \sim \mathcal{CN}(0, 1)$. The ground devices have single antenna and the communication channels follow Rayleigh fading. $\tilde{\mathbf{h}}_{ab}$ and $\tilde{\mathbf{h}}_{ae}$ follow the small-scale fading with a mean of 0 and variance of 1. Thus, the channel from Alice to Bob and Eve are denoted as

$$\begin{cases} h_{ab}[n] = \sqrt{\rho_0 d_{ab}^{-\alpha_2}}\tilde{\mathbf{h}}_{ab}[n], \\ h_{ae}[n] = \sqrt{\rho_0 d_{ae}^{-\alpha_2}}\tilde{\mathbf{h}}_{ae}[n], \end{cases} \quad (7)$$

where

$$\begin{cases} d_{ab} = \sqrt{\left(x_A - x_B\right)^2 + \left(y_A - y_B\right)^2}, \\ d_{ae} = \sqrt{\left(x_A - x_E\right)^2 + \left(y_A - y_E\right)^2}, \end{cases} \tag{8}$$

d_{ab} and d_{ae} represent the distance between Alice and Bob and the distance between Alice and eavesdropper, respectively. α_2 is path loss exponent of terrestrial communication. $\tilde{\mathbf{h}}_{ab}$ and $\tilde{\mathbf{h}}_{ae}$ follow independently and identically distribution.

When the Alice sends privacy information, the received signal at Bob and Eve are denoted as

$$\begin{cases} y_b\left[n\right] = \sqrt{P_a} \cdot \mathbf{h}_b\left[n\right] \cdot x_a\left[n\right] + n_b\left[n\right], \\ y_e\left[n\right] = \sqrt{P_a} \cdot \mathbf{h}_e\left[n\right] \cdot x_a\left[n\right] + n_e\left[n\right], \end{cases} \tag{9}$$

where $\mathbf{h}_b\left[n\right] = h_{ab}\left[n\right] + \mathbf{h}_{ub}^H\left[n\right]\mathbf{\Phi}_n\mathbf{h}_{ru}\left[n\right]$, and $\mathbf{h}_e\left[n\right] = h_{ae}\left[n\right] + \mathbf{h}_{ue}^H\left[n\right]\mathbf{\Phi}_n\mathbf{h}_{ru}\left[n\right]$. $x_a\left[n\right]$ is the transmit signal of Alice, P_a is the Alice's transmit power, $n_b\left[n\right]$ and $n_e\left[n\right]$ are the interference noise in the n-th time slot at Bob and Eve. The expression of RIS phase shift $\mathbf{\Phi}_n$ is $\mathbf{\Phi}_n = diag\left\{e^{j\varphi_1[n]}, \cdots, e^{j\varphi_M[n]}\right\}, \varphi \in [0, 2\pi]$, where φ_i is the phase shift corresponding to each RIS reflective element.

B. Problem Formulation

The communication links from Alice to Bob and Eve consists of direct and indirect links. Thus, the information rates at Bob and Eve can be derived as

$$\begin{cases} R_b\left[n\right] = \log_2\left(1 + \frac{\left|h_{ab}[n] + \mathbf{h}_{ub}^H[n]\mathbf{\Phi}_n\mathbf{h}_{au}[n]\right|^2}{\sigma^2}\right), \\ R_e\left[n\right] = \log_2\left(1 + \frac{\left|h_{ae}[n] + \mathbf{h}_{ue}^H[n]\mathbf{\Phi}_n\mathbf{h}_{au}[n]\right|^2}{\sigma^2}\right), \end{cases} \tag{10}$$

where σ^2 is the noise power.

The secrecy rate is $R_{s,r}\left[n\right] = \left(R_b\left[n\right] - R_e\left[n\right]\right)^+$, where $(x)^+ = \max(0, x)$. The total secrecy rate optimization problem can be expressed as

$$\mathbf{P1}: \quad \max_{\mathbf{\Phi}, \mathbf{Z}} \sum_{n=0}^{N} R_{s,r}\left[n\right] \tag{11a}$$

$$s.t. \quad \varphi_m \in [0, 2\pi], m = 1, 2, ..., M, \tag{11b}$$

$$\mathbf{Z}[1] = \mathbf{Z}_{\text{initial}}, \mathbf{Z}[n] \in X \times Y, n \in \{2, \ldots, N\}, \tag{11c}$$

$$||\mathbf{Z}[n+1] - \mathbf{Z}[n]||^2 \leq \left(\frac{TV_{\max}}{N}\right)^2, n \in \{2, \ldots, N\}, \tag{11d}$$

where $V_{\max}$ is UAV's maximum velocity. T/N indicates the time for each time slot. The constraint (11c) indicates that the initial position of the UAV is fixed and it cannot move beyond the given region ($X \times Y$). And the constraint (11d) represents the maximum horizontal displacement that the UAV can move in adjacent time slots.

III. The Phase Shift and UAV's Trajectory Optimization

A. Phase shift Optimization

We first fix UAV trajectory $\mathbf{Z}$, and denote the RIS phase shift optimization problem as

$$\mathbf{P2}: \quad \max_{\mathbf{\Phi}_n} R_{s,r}\left[n\right] \tag{12a}$$

$$s.t. \quad \varphi_m \in [0, 2\pi], \tag{12b}$$

where the secrecy rate can be denoted as

$$R_{s,r}[n] = \log_2\left(\frac{\sigma^2 + \left|h_{ab}\left[n\right] + \mathbf{h}_{ub}^H\left[n\right]\mathbf{\Phi}_n\mathbf{h}_{au}\left[n\right]\right|^2}{\sigma^2 + \left|h_{ae}\left[n\right] + \mathbf{h}_{ue}^H\left[n\right]\mathbf{\Phi}_n\mathbf{h}_{au}\left[n\right]\right|^2}\right). \tag{13}$$

Then, the RIS phase shift optimization problem is restructured as

$$\mathbf{P3}: \quad \max_{\mathbf{\Phi}_n} \frac{\sigma^2 + \left|h_{ab}\left[n\right] + \mathbf{h}_{ub}^H\left[n\right]\mathbf{\Phi}_n\mathbf{h}_{au}\left[n\right]\right|^2}{\sigma^2 + \left|h_{ae}\left[n\right] + \mathbf{h}_{ue}^H\left[n\right]\mathbf{\Phi}_n\mathbf{h}_{au}\left[n\right]\right|^2} \tag{14a}$$

$$s.t. \quad \varphi_m \in [0, 2\pi], m = 1, 2, ..., M, \tag{14b}$$

We define $\mathbf{s}^H\left[n\right] = [\varphi_1[n], \varphi_2[n], \ldots, \varphi_M[n]]$. From the theorem $\mathbf{x}^H\mathbf{\Phi}_n y = \mathbf{s}^H diag\left\{\mathbf{x}^H\right\}\mathbf{y}$, the problem can be formulated as

$$\min_{\mathbf{\Phi}_n} \frac{\sigma^2 + \left|h_{ae}\left[n\right] + \mathbf{s}^H\left[n\right] diag\left\{\mathbf{h}_{ue}^H\left[n\right]\right\}\mathbf{h}_{au}\left[n\right]\right|^2}{\sigma^2 + \left|h_{ab}\left[n\right] + \mathbf{s}^H\left[n\right] diag\left\{\mathbf{h}_{ub}^H\left[n\right]\right\}\mathbf{h}_{au}\left[n\right]\right|^2}, \tag{15}$$

where

$$\begin{cases} \mathbf{h}_{ub}^H\left[n\right]\mathbf{\Phi}_n\mathbf{h}_{au}\left[n\right] = \mathbf{s}^H\left[n\right] diag\left\{\mathbf{h}_{ub}^H\left[n\right]\right\}\mathbf{h}_{au}\left[n\right], \\ \mathbf{h}_{ue}^H\left[n\right]\mathbf{\Phi}_n\mathbf{h}_{au}\left[n\right] = \mathbf{s}^H\left[n\right] diag\left\{\mathbf{h}_{ue}^H\left[n\right]\right\}\mathbf{h}_{au}\left[n\right], \end{cases} \tag{16}$$

The problem (15) is a nonlinear fractional programming problem, and we transform this optimization problem into a number of subproblems containing parameters [11]. In the r-th iteration, we introduce a non-negative value to represent the problem as

$$\min_{\mathbf{s[n]}} \sigma^2 + \left|h_{ae}\left[n\right] + \mathbf{s}^H\left[n\right] diag\left\{\mathbf{h}_{ue}^H\left[n\right]\right\}\mathbf{h}_{au}\left[n\right]\right|^2 \tag{17}$$

$$- \eta^{(r-1)}\left(\sigma^2 + \left|h_{ab}\left[n\right] + \mathbf{s}^H\left[n\right] diag\left\{\mathbf{h}_{ub}^H\left[n\right]\right\}\mathbf{h}_{au}\left[n\right]\right|^2\right),$$

where

$$\eta^{(r)} = \frac{\sigma^2 + \left|h_{ae}\left[n\right] + \mathbf{s}^{(r)H}[n] diag\left\{\mathbf{h}_{ue}^H\left[n\right]\right\}\mathbf{h}_{au}\left[n\right]\right|^2}{\sigma^2 + \left|h_{ab}\left[n\right] + \mathbf{s}^{(r)H}[n] diag\left\{\mathbf{h}_{ub}^H\left[n\right]\right\}\mathbf{h}_{au}\left[n\right]\right|^2}. \tag{18}$$

η has an initial value of 0. $\eta^{(r-1)}$ denotes the value of η in the $(r-1)$-th iteration.

Note that the objective function (17) is still non-convex, which cannot be directly solved by convex optimization. Therefore, we intend to find an objective upper bound of (15) as (19) at the top of the next page. In (19),

$$\begin{cases} \mathbf{A}\left[n\right] = \left|\left(diag\left\{\mathbf{h}_{ue}^H\left[n\right]\right\}\mathbf{h}_{au}\left[n\right]\right)\right|^2 \\ \qquad\qquad -\eta\left|\left(diag\left\{\mathbf{h}_{ue}^H\left[n\right]\right\}\mathbf{h}_{au}\left[n\right]\right)\right|^2, \\ \mathbf{B}\left[n\right] = h_{ae}^*\left[n\right] diag\left\{\mathbf{h}_{ue}^H\left[n\right]\right\}\mathbf{h}_{au}\left[n\right] \\ \qquad\qquad -\eta h_{ae}^*\left[n\right] diag\left\{\mathbf{h}_{ue}^H\left[n\right]\right\}\mathbf{h}_{au}\left[n\right], \\ c\left[n\right] = \sigma^2 + \left|h_{ae}\left[n\right]\right|^2 - \eta\left|h_{ab}\left[n\right]\right|^2 - \eta\sigma^2. \end{cases} \tag{20}$$

$$\begin{aligned}&\sigma^2+\left|h_{ae}[n]+\mathbf{s}^H[n]\,diag\left\{\mathbf{h}_{ue}^H[n]\right\}\mathbf{h}_{au}[n]\right|^2-\eta^{r-1}\left(\sigma^2+\left|h_{ab}[n]+\mathbf{s}^H[n]\,diag\left\{\mathbf{h}_{ub}^H[n]\right\}\mathbf{h}_{au}[n]\right|^2\right)\\&=(1-\eta)\sigma^2+\mathbf{s}^H[n]\,\mathbf{A}[n]\,\mathbf{s}[n]-2\mathrm{Re}\left\{\mathbf{s}^H[n]\,\mathbf{B}[n]\right\}+\left|h_{ae}[n]\right|^2-\eta\left|h_{ab}[n]\right|^2\\&\le\lambda_{max}\left(\mathbf{A}[n]\left|s[n]\right|^2\right)-2\mathrm{Re}\left\{\mathbf{s}^H[n]\,\mathbf{B}[n]\right\}+c[n],\end{aligned}\tag{19}$$

Then, we abbreviate the RIS phase shift optimization problem as

$$\mathbf{P4}:\min_{s[n]}\lambda_{max}\left(\mathbf{A}[n]\,s[n]^2\right)-2\Re\left\{\mathbf{u}^H[n]\,\mathbf{B}[n]\right\}+c[n]\tag{21a}$$

$$s.t.\quad\left|e^{\varphi_m[n]}\right|=1.\tag{21b}$$

λ_{max} represents the maximum eigenvalue corresponding to the matrix. We can derive that $||s[n]||^2=M$ due to the existence of the constraint (21b) ($\left|e^{\varphi_m[n]}\right|=1$). Thus $\lambda_{max}\left(\mathbf{A}[n]\,||\mathbf{s}[n]||^2\right)$ is simply constant. Specifically, the RIS optimal phase shift can be obtained by maximizing the second half of the minus sign of this optimization problem. Then, the mathematical expression of RIS optimal phase shift is denoted as

$$\mathbf{\Phi}_n=diag[e^{j\arg(\mathbf{B}_1[n])},...,e^{j\arg(\mathbf{B}_M[n])}].\tag{22}$$

B. UAV Trajectory Optimization

According to the obtained RIS optimal phase shift $\mathbf{\Phi}_n$, the UAV trajectory optimization problem is

$$\mathbf{P4}:\quad\max_{\mathbf{Z}}\frac{\sigma^2+\left|h_{ab}[n]+\mathbf{h}_{ub}^H[n]\,\mathbf{\Phi}_n\mathbf{h}_{au}[n]\right|^2}{\sigma^2+\left|h_{ae}[n]+\mathbf{h}_{ue}^H[n]\,\mathbf{\Phi}_n\mathbf{h}_{au}[n]\right|^2}\tag{23a}$$

$$\mathbf{Z}[1]=\mathbf{Z}_{\text{initial}},\mathbf{Z}[n]\in X\times Y,\tag{23b}$$

$$||\mathbf{Z}[n+1]-\mathbf{Z}[n]||^2\le\left(\frac{T}{N}\cdot V_{\max}\right)^2,n\in\{2,\ldots,N\}.\tag{23c}$$

We find that the non-convexity of objective function in (23a), and can be turned into a convex optimization problem after some mathematical transformations. Specifically, the information rate $R_b[n]$ and $R_e[n]$ are neither concave nor convex. For the Bob, we transform the mathematical form of its received signal,

$$\begin{aligned}&\left|h_{ab}[n]+\mathbf{h}_{ub}^H[n]\,\mathbf{\Phi}_n\mathbf{h}_{au}[n]\right|^2\\&=\left|h_{ab}[n]\right|^2+d_{au}^{-\frac{\alpha}{2}}d_{ub}^{-\frac{\alpha}{2}}D_b[n]+d_{au}^{-\alpha}d_{ub}^{-\alpha}E_b[n],\end{aligned}\tag{24}$$

where $\mathbf{g}_b[n]=\mathbf{h}_{ub}^H[n]\,\mathbf{\Phi}_n$, $D_b[n]$ and $E_b[n]$ are constant coefficients, which are defined as

$$\begin{cases}D_b[n]=2\mathrm{Re}\left\{\mathbf{g}_b[n]\,\tilde{\mathbf{h}}_{ab}[n]\right\},\\E_b[n]=\mathbf{g}_b[n]\,\mathbf{h}_{au}[n]\,\mathbf{h}_{au}^H[n]\,\mathbf{g}_b^H[n].\end{cases}\tag{25}$$

Similarly, we can transform the signal expression at the eavesdropper into the following form

$$\begin{aligned}&\left|h_{ae}[n]+\mathbf{h}_{ue}^H[n]\,\mathbf{\Phi}_n\mathbf{h}_{au}[n]\right|^2\\&=\left|h_{ae}[n]\right|^2+d_{ue}^{-\frac{\alpha}{2}}d_{au}^{-\frac{\alpha}{2}}D_e[n]+d_{ue}^{-\alpha}d_{au}^{-\alpha}E_e[n],\end{aligned}\tag{26}$$

where $\mathbf{g}_e[n]=\mathbf{h}_{ue}^H[n]\,\mathbf{\Phi}_n$, $D_b[n]$ and $E_b[n]$ are denoted as

$$\begin{cases}D_e[n]=2\mathrm{Re}\left\{\mathbf{g}_e[n]\,\tilde{\mathbf{h}}_{ae}[n]\right\}\\E_e[n]=\mathbf{g}_e[n]\,\mathbf{h}_{au}[n]\,\mathbf{h}_{au}^H[n]\,\mathbf{g}_e^H[n].\end{cases}\tag{27}$$

The objective function after the above transformations is reconstructed as

$$\max_{\mathbf{Z}}\frac{\sigma^2+\left|h_{ab}[n]\right|^2+d_{au}^{-\frac{\alpha}{2}}d_{ub}^{-\frac{\alpha}{2}}D_b[n]+d_{au}^{-\alpha}d_{ub}^{-\alpha}E_b[n]}{\sigma^2+\left|h_{ae}[n]\right|^2+d_{au}^{-\frac{\alpha}{2}}d_{ue}^{-\frac{\alpha}{2}}D_e[n]+d_{au}^{-\alpha}d_{ue}^{-\alpha}E_e[n]},\tag{28}$$

where the UAV position is one of the objectives, and the corresponding variable is d_{ui} ($i\in\{a,b,e\}$). To obtain the approximate solution of the problem (28), two auxiliary variables $u,v,(u\ge0,v\ge0)$ are introduced as follows

$$\begin{cases}d_{au}^{-\frac{\alpha}{2}}d_{ub}^{-\frac{\alpha}{2}}\ge u\Rightarrow d_{au}d_{ub}\le u^{-\frac{2}{\alpha}},\\d_{au}^{-\frac{\alpha}{2}}d_{ue}^{-\frac{\alpha}{2}}\le v\Rightarrow d_{au}d_{ue}\ge v^{-\frac{2}{\alpha}}.\end{cases}\tag{29}$$

The non-convex constraint (29) can be reconstructed as $d_{au}d_{ub}\le u^{-\frac{2}{\alpha}}$ and $d_{au}d_{ue}\ge v^{-\frac{2}{\alpha}}$. Specifically, the first-order Taylor expansion is used for converting their mathematical form to

$$\begin{aligned}d_{ru}d_{ub}&=\frac{1}{2}\left((d_{au}+d_{ub})^2-d_{au}^2-d_{ub}^2\right)\\&\le\tfrac{1}{2}\left((d_{au}+d_{ub})^2-d_{au}^2-d_{ub}^2\right)\\&\quad-(2\mathbf{Z}_0-\mathbf{Z}_a-\mathbf{Z}_b)^T(\mathbf{Z}-\mathbf{Z}_0)=\Xi.\end{aligned}\tag{30}$$

Then the objective upper bound can be obtained. The left side of the inequality can be regarded as approximating at u_0.

$$u^{-\frac{2}{\alpha}}\ge u_0^{-\frac{2}{\alpha}}-\frac{2}{\alpha}u_0{}^{\frac{2}{\alpha}-1}(u-u_0).\tag{31}$$

Analogously, we can also transform the constraint (30) to

$$\begin{aligned}d_{au}d_{ue}&\ge\tfrac{1}{2}(d_{au}(\mathbf{Z}_0)+d_{ue}(\mathbf{Z}_0))^2\\&\quad-\tfrac{1}{2}\left(d_{au}^2(\mathbf{Z})+d_{ub}^2(\mathbf{Z})\right)+X(\mathbf{Z})=\Psi,\end{aligned}\tag{32}$$

where

$$\begin{aligned}X(\mathbf{Z})&=(d_{au}(\mathbf{Z}_0)+d_{ue}(\mathbf{Z}_0))\\&\quad\cdot\left(\tfrac{\mathbf{Z_0}-\mathbf{Z}_r}{d_{au}(\mathbf{Z_0})}+\tfrac{\mathbf{Z_0}-\mathbf{Z}_e}{d_{ue}(\mathbf{Z_0})}\right)^T(\mathbf{Z}-\mathbf{Z}_0),\end{aligned}\tag{33}$$

can be seen as an approximation at $\mathbf{Z_0}$. We denote the denominator of the optimization problem (28) as $\Upsilon=\left|h_{ab}[n]\right|^2+$

$uD_b[n] + u^2 E_b[n]$, and then reformulate the UAV trajectory optimization problem as

$$\mathbf{P5}: \quad \min_{u[n],v[n],\mathbf{Z},\Upsilon} \frac{|h_{ab}[n]|^2 + vD_e[n] + v^2E_e[n]}{\Upsilon} \tag{34a}$$

$$s.t. \quad \Upsilon \geq 0, \tag{34b}$$

$$\Xi \leq u_0^{-\frac{2}{\alpha}} - \frac{2}{\alpha} u_0^{\frac{2}{\alpha}-1}(u-u_0), \tag{34c}$$

$$\Psi \geq v^{-\frac{2}{\alpha}}, \tag{34d}$$

$$|h_{ab}[n]|^2 + u_0 D_b[n] + u_0^2 E_b[n] + (D_b[n] + 2u_0E_b[n])(u-u_0) \geq \Upsilon. \tag{34e}$$

The DQN algorithm is conceived for the UAV trajectory optimization. DQN is based on reinforcement learning algorithm that a neural network is used to learn the Q-value function. The function maps states and actions to Q-values, representing the expected reward in a specific state by performing that action. Discretising UAV trajectory in each time slot is core of DQN algorithm, and we use a dual neural network with a current network (θ) and a target network (θ^-). The initial parameters are set identically ($\theta = \theta^-$). For the state s_n and action a_n, the value of Q can be expressed as

$$Q(s_n, a_n) = r^n + \gamma \max(s^{n+1}, a^{n+1}), \tag{35}$$

where the discount factor is γ ($\gamma \in [0,1)$). The reward is r. In the n-th time slot, the reward is set in two cases: $r^n = R_{s,r}[n]$ when the UAV is within the flight area, and $r^n = R_{s,r}[n]/100$ when the UAV flies beyond given area.

For the UAV motion, we divide the given flight area into a grid-like shape. In the horizontal direction, UAV can fly in four directions: east, south, west and north, and can only move up, down or maintain original altitude in the vertical direction. Furthermore, UAV can only fly to the adjacent horizontal cells and altitude levels within adjacent time slot, which can be represented as

$$\boldsymbol{L}_{n+1} = \boldsymbol{L}_n + \boldsymbol{l}_n, \boldsymbol{H}_{n+1} = \boldsymbol{H}_n + \boldsymbol{h}_n, \tag{36}$$

where $\boldsymbol{l}_n \in \{(x_n, 0), (-x_n, 0), (0, y_n), (0, -y_n)\}$, and $\boldsymbol{h}_n \in \{h_n, 0, -h_n\}$. The reward r and Q value are stored in the experience pool, and trained iteratively to maximize the secrecy rate, thus obtaining optimized UAV trajectory. The DQN algorithm framework is shown in Fig. 2.

IV. Simulation Experiments

In this section, we emulate the communication network's security performance. In the simulation, the transmission power of Alice is set to $0.2W$, the RIS reflective elements $M = 100$. The UAV flight time $T = 240s$, with a total of $N = 2000$ time slots. The noise density is -160 dBm/Hz, the initial position of UAV is $[50, 50, 180]$, and the horizontal position of the Alice, Bob and eavesdropper are $[350, 920]$, $[610, 900]$ and $[810, 940]$. In addition, we also introduce other benchmark schemes for comparison with proposed scheme. The specific parameters used in the simulation are outlined in Table I.

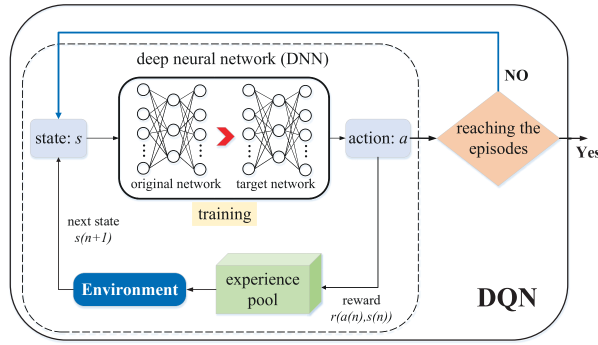

Fig. 2. DQN algorithm framework.

TABLE I
Simulation Parameters.

Parameter	Value
path loss at $d = 1m$, ρ_0	-40 dB
path loss, α_1, α_2	2
UAV flight region, $X \times Y$	1000 $\times$ 1000 m
UAV maximum velocity, $V_{\max}$	10 m/s
initial UAV altitude, H_{uav}	100 m
UAV flight altitude range	(30m, 210m)
noise density, σ^2	-160 dBm/Hz

Fig. 3 shows the UAV's 3D trajectory for the three different schemes. The blue, red, and green lines in the figure correspond to the proposed scheme, without RIS (Algorithm 1), and without RIS phase shift optimization (Algorithm 2), respectively. In Fig. 3, the UAV gradually approaches the legitimate receiver Bob, which allows for better information transmission to increase the secrecy rate. The proposed scheme achieves the shorter distance to the legitimate receiver, enabling faster movement toward Bob. Simulation results substantiate that the proposed scheme is more effective in improvings secrecy rate compared with the two benchmark schemes.

In Fig. 4, we plot the tendency of secrecy capability of the network with episodes. As the number of training sessions increases, the secrecy performance improves. The proposed scheme for UAV trajectory optimization adapts more rapidly to the surrounding environment through the experience pool, thus guiding UAV to choose the next movement and gradually move to Bob. The secrecy rate is effectively increased, and convergence is faster. Compared to Algorithm 1 (without RIS), the RIS-assisted communication increases the signal multiplexing gain by adding additional communication paths and channel subspaces. Furthermore, secrecy rate is improved with RIS phase shift optimization.

Fig. 5 depicts the secrecy rate performance for the proposed scheme and the two benchmark schemes. As we can see, the secrecy rate increases as T increases, but eventually levels off. Because the larger T is, the longer the UAV stays near the legitimate receiver Bob. The secrecy rate that without UAV trajectory optimization is significantly lower than the proposed scheme. Without trajectory optimization (Algorithm 3), the UAV moves away from Bob and Eve, resulting in a lower

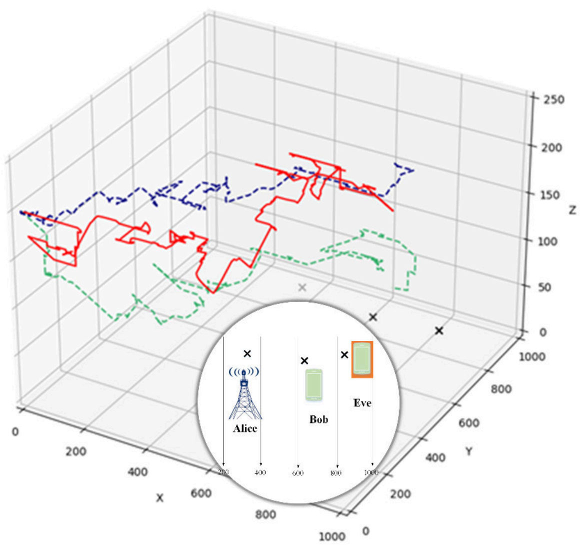

Fig. 3. The 3D UAV trajectory.

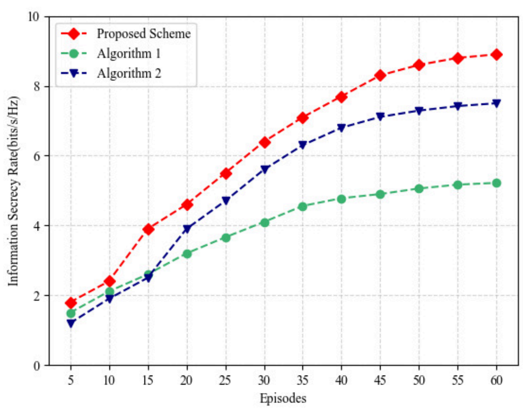

Fig. 4. Secrecy rate VS episodes.

secrecy rate. Additionally, the assistance of RIS effectively prevents eavesdropping compared to the scheme without RIS, while providing better service to the legitimate receiver.

V. Conclusion

In this paper, we investigated a RIS-assisted secure communication network. For maximizing secrecy rate, we decoupled the optimization problem into two subproblems: RIS phase shifts and UAV trajectory optimization. For RIS phase shifts optimization, the fractional programming was designed. Subsequently, we used the DQN algorithm to obtain the optimal UAV trajectory. The secrecy rate of the proposed scheme was increased by 18.7% compared with the two benchmark schemes.

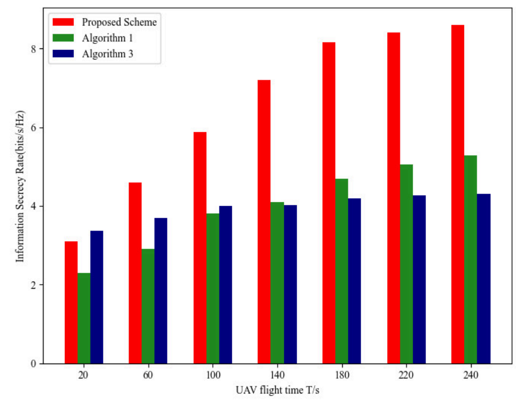

Fig. 5. Secrecy rate for three schemes.

References

[1] S. Chen, S. Sun and S. Kang, "System integration of terrestrial mobile communication and satellite communication —the trends, challenges and key technologies in B5G and 6G," *China Communications.*,vol. 17, no. 12, pp. 156-171, Dec. 2020.

[2] Z. Zhang, J. Tian, D. Wang, J. Qiao and T. Li, "TD3-based Joint UAV Trajectory and Power optimization in UAV-Assisted D2D Secure Communication Networks," *2022 IEEE 96th Vehicular Technology Conference (VTC2022-Fall).*, London, United Kingdom, 2022, pp. 1-5.

[3] Y. Jiang and J. Zhu, "Three-dimensional trajectory optimization for secure UAV-enabled cognitive communications," *China Communications.*,vol. 18, no. 12, pp. 285-296.

[4] W. Lv, J. Bai, Q. Yan and H. M. Wang, "RIS-Assisted Green Secure Communications: Active RIS or Passive RIS?," *IEEE Wireless Communications Letters.*,vol. 12, no. 2, pp. 237-241, Feb. 2023.

[5] X. Pang, N. Zhao, J. Tang, C. Wu, D. Niyato and K. -K. Wong, "IRS-Assisted Secure UAV Transmission via Joint Trajectory and Beamforming Design," *IEEE Transactions on Communications.*,vol. 70, no. 2, pp. 1140-1152, Feb. 2022.

[6] K. K. Nguyen, A. Masaracchia, V. Sharma, H. V. Poor and T. Q. Duong, "RIS-Assisted UAV Communications for IoT With Wireless Power Transfer Using Deep Reinforcement Learning," *IEEE Journal of Selected Topics in Signal Processing.*,vol. 16, no. 5, pp. 1086-1096, Aug. 2022.

[7] H. Mei, K. Yang, Q. Liu and K. Wang, "3D-Trajectory and Phase-Shift Design for RIS-Assisted UAV Systems Using Deep Reinforcement Learning," *IEEE Transactions on Vehicular Technology.*,vol. 71, no. 3, pp. 3020-3029, March 2022.

[8] X. Tang, D. Wang, R. Zhang, Z. Chu and Z. Han, "Jamming Mitigation via Aerial Reconfigurable Intelligent Surface: Passive Beamforming and Deployment Optimization," *IEEE Transactions on Vehicular Technology.*,vol. 70, no. 6, pp. 6232-6237, June 2021.

[9] H. Long et al., "Joint Trajectory and Passive Beamforming Design for Secure UAV Networks with RIS," *2020 IEEE Globecom Workshops.*,Taipei, Taiwan, 2020, pp. 1-6.

[10] X. Song, Y. Zhao, Z. Wu, Z. Yang and J. Tang, "Joint Trajectory and Communication Design for IRS-Assisted UAV Networks," *IEEE Wireless Communications Letters.*,vol. 11, no. 7, pp. 1538-1542, July 2022.

[11] J. Zhang, S. Chen, F. Wang, S. X. Ng, R. G. Maunder and L. Hanzo, "Priority-Aware Secure Precoding Based on Multi-Objective Symbol Error Ratio Optimization," *IEEE Transactions on Communications.*,vol. 69, no. 3, pp. 1912-1929, March 2021.

[12] Y. Li, H. Zhang, K. Long and A. Nallanathan, "Exploring Sum Rate Maximization in UAV-Based Multi-IRS Networks: IRS Association, UAV Altitude, and Phase Shift Design," *IEEE Transactions on Communications.*, vol. 70, no. 11, pp. 7764-7774, Nov. 2022.

[13] P. Chen, F. Xiao, L. Yang, T. A. Tsiftsis and H. Liu, "Covert Beamforming Design for Active RIS-Assisted NOMA-ISAC Systems," *2023 IEEE Globecom Workshops (GC Wkshps).*, Kuala Lumpur, Malaysia, 2023, pp. 1141-1146.